



HAL
open science

Accurate absolute frequency measurement of the S(2) transition in the fundamental band of H₂ near 2.03 μm

D. Mondelain, L. Boux de Casson, H. Fleurbaey, S. Kassi, A. Campargue

► To cite this version:

D. Mondelain, L. Boux de Casson, H. Fleurbaey, S. Kassi, A. Campargue. Accurate absolute frequency measurement of the S(2) transition in the fundamental band of H₂ near 2.03 μm. *Physical Chemistry Chemical Physics*, 2023, 25 (34), pp.22662-22668. 10.1039/d3cp03187j . hal-04221902

HAL Id: hal-04221902

<https://hal.science/hal-04221902v1>

Submitted on 19 Oct 2023

HAL is a multi-disciplinary open access archive for the deposit and dissemination of scientific research documents, whether they are published or not. The documents may come from teaching and research institutions in France or abroad, or from public or private research centers.

L'archive ouverte pluridisciplinaire **HAL**, est destinée au dépôt et à la diffusion de documents scientifiques de niveau recherche, publiés ou non, émanant des établissements d'enseignement et de recherche français ou étrangers, des laboratoires publics ou privés.

1 **Accurate absolute frequency measurement of the S(2) transition**
2 **in the fundamental band of H₂ near 2.03 μm**
3

4 D. Mondelain*, L. Boux de Casson, H. Fleurbaey, S. Kassi, A. Campargue

5
6 *Univ. Grenoble Alpes, CNRS, LIPhy, 38000 Grenoble, France*
7
8
9
10
11
12
13
14
15
16
17
18
19
20
21
22
23

24 *Corresponding author: didier.mondelain@univ-grenoble-alpes.fr; LIPhy, Bat. E, 140 rue de la
25 Physique, 38400 Saint-Martin d'Hères (France).
26
27
28
29
30

31 **Key words**

32 Frequency metrology; H₂; hydrogen; CRDS; frequency comb
33

34

35 **Abstract**

36 Series of spectra of the quadrupolar electric S(2) transition of H₂ in the 1-0 band near 4917 cm⁻¹
37 has been recorded at seven pressure values between 2 and 100 Torr. Comb-referenced cavity ring
38 down spectroscopy technique (CR-CRDS) was used for the recordings of this very weak transition.
39 The accuracy of the spectra frequency axis is achieved by linking the CRDS setup to an optical
40 frequency comb referenced to a GPS-referenced 10 MHz rubidium clock. Applying a multi-spectrum
41 fit procedure to the seven averaged spectra with a quadratic Speed Dependence Nelkin-Ghatak
42 profile, the transition frequency is determined ($\nu_0 = 147\,408\,142\,357$ kHz) with an uncertainty of 150
43 kHz ($\sim 1 \times 10^{-9}$ in relative). This represents the smallest uncertainty achieved so far for a transition in
44 the fundamental band of H₂. The experimental frequency reported in this work is 1.53 MHz higher
45 than the best-to-date theoretical value. This difference represents 1.5 times the 1 σ -uncertainty
46 (about 1 MHz) on the calculated frequency. The measurements also allow for the determination of
47 the absolute intensity value of the S(2) line which shows an agreement with the *ab initio* value at the
48 per mil level. In addition, the cross section of the collision induced absorption (CIA) underlying the
49 S(2) line is accurately retrieved from the quadratic pressure dependence of the baseline level of the
50 recorded spectra.

51 1. Introduction

52 Di-hydrogen and its isotopologues being the simplest neutral molecular systems, their
53 rovibrational energy levels in the electronic ground state can be accurately determined by theoretical
54 calculations [1]. To achieve a high degree of accuracy, these calculations include corrections to the
55 Born-Oppenheimer approximation, as well as high order quantum electrodynamics (QED) corrections
56 and finite nuclear size effects. Comparison of the theoretical values with accurate experimental
57 measurements provides a strong test of the QED theory which fully describes the molecular systems
58 and puts a higher limit on the coupling strength of a potential 5th force [2,3]. Because H₂ and D₂ are
59 homonuclear molecules, their ro-vibrational absorption spectrum consists only in very weak electric-
60 quadrupole transitions. This results in a real experimental challenge to measure the absolute
61 frequency of such weak transitions with accuracy competing with that reported for the theoretical
62 value. As an example, the strongest transition in the 1-0 fundamental band of H₂ has a line intensity
63 of 3.2×10^{-26} cm molecule⁻¹ at 296 K [4] and the minimal required uncertainty should be below 1 MHz.
64 Thanks to the presence of a weak electric dipole moment, HD isotopologue possesses transitions
65 which are stronger than the H₂ and D₂ quadrupolar transitions, making it a better choice for
66 metrological frequency determination. Nevertheless, to check potential (vibrational, isotopologue)
67 dependence of the *ab initio* calculations, it is important to have at disposal the largest number of
68 accurate experimental frequency measurements as possible for the different isotopologues,
69 vibrational bands and transitions. Up to now, such measurements are relatively scarce (5,6 and
70 references herein). Most of them were obtained by Doppler limited spectroscopy. Saturation
71 spectroscopy has been applied to HD transitions but with the drawback of an hyperfine structure
72 limiting the final accuracy on the line centre determination [7,8,9,10,11]. Very recently, Cozijn and
73 co-workers achieved the feat of saturating the S(0) transition in the 2-0 band of H₂ with the NICE-
74 OHMS technique and a H₂ gas sample at 72 K [12] and reported a transition frequency uncertainty of
75 8 kHz, in agreement with the frequency measured with a 60 kHz uncertainty in Doppler regime by
76 comb-referenced cavity ring down spectroscopy (CR-CRDS) [5]. This latter work, also including the
77 frequency determination of five other transitions in the 2-0 band, evidenced a systematic
78 underestimation of about 2.58 MHz of the most recent calculated H₂ frequencies, about twice their
79 claimed uncertainties. Apart these six transition frequencies measured with a sub-MHz uncertainty in
80 the 2-0 band, only the Q(1) transition in the 1-0 band has been measured with such a level of
81 accuracy [6]. The Q(1) 1-0 transition frequency near 4155 cm^{-1} was very recently reported with an
82 uncertainty of 310 kHz using stimulated Raman scattering metrology [6]. The measured value was
83 found 0.84 MHz larger than predicted by theory. In order to extend the measurements in the 1-0
84 fundamental band, we consider here the S(2) transition ($\nu_0 = 4917.006312 \text{ cm}^{-1}$ [4]; $S = 4.577 \times 10^{-27}$
85 cm/molecule [13]). The S(2) transition frequency is presently derived from series of spectra recorded

86 with a CRDS spectrometer referenced to an optical frequency comb (OFC). The setup and the
 87 acquisition procedure are detailed in the next section, followed by a description of the adopted
 88 multi-spectrum fit procedure (Section 3) and the budget error (Section 4). Retrieved absolute
 89 frequency and line shape parameters are then discussed and compared to previous works before
 90 concluding remarks (Section 5).

91 **2. Setup and acquisition procedure**

92 *2.1. Experimental setup*

93 The comb-referenced cavity ring down spectrometer used in this work is identical to the one
 94 described in [14]. Briefly, it consists in an extended cavity diode laser (ECDL) which is coupled into a
 95 temperature stabilized high finesse cavity (TS-HFC) [15,16]. The cavity is made of two high reflectivity
 96 mirrors (with a reflection coefficient $R > 99.99\%$ over the 1950-2250 nm range) separated by 45.5 cm.
 97 Periodic resonances between the laser light and a cavity mode are achieved by applying a voltage
 98 triangular ramp on the PZT tube on which the output cavity mirror is installed. At each resonance,
 99 ring-down (RD) events are detected by a photodiode after switching off the injection of photons with
 100 an acousto-optic modulator (AOM). The ring down time at frequency ν , $\tau(\nu)$, is derived from a fit of
 101 the RD event with a purely decreasing exponential function. The extinction coefficient, $\alpha(\nu)$, is thus
 102 retrieved using Eq. (1):

$$103 \quad \alpha(\nu) = \frac{n}{c\tau(\nu)} - \frac{1-R(\nu)}{L_{cav}} \quad (1)$$

104 Where c is the speed of light, n is the refractive index of the absorbing gas, $R(\nu)$ is the reflectivity of
 105 the mirrors and L_{cav} is the cavity length. Typical RD times of the evacuated cell are $\tau \sim 51 \mu\text{s}$ at 4917
 106 cm^{-1} .

107 The rest of the ECDL light is mixed with the output of an OFC to obtain a beat note (BN) signal
 108 detected with a fast photodiode. After acquisition of the signal, the beat note frequency, f_{BN} , is
 109 derived allowing retrieving the absolute frequency associated to the RD event from Eq. (2):

$$110 \quad \nu = nf_{rep} + f_{CEO} + f_{BN} - f_{AOM} \quad (2)$$

111 Where the repetition rate, $f_{rep} = 250 \text{ MHz}$, and the carrier-envelop offset, $f_{CEO} = -20 \text{ MHz}$, of the OFC are
 112 referenced to a 10 MHz rubidium frequency standard phase-locked to a GPS timing receiver. The
 113 sinusoidal wave of frequency $f_{AOM} = 94.15 \text{ MHz}$ applied to the AOM is generated with a direct digital
 114 synthesizer (DDS) also referenced to the 10 MHz frequency standard as well as the fast BN
 115 acquisition board. Note that the minus sign for f_{AOM} is due to the fact that the beam of order -1 is
 116 used. The tooth number, n , is determined with a commercial wavelength meter (HighFinesse WS7-60
 117 IR-II). At the end, an absolute frequency known with an uncertainty of $\sim 200 \text{ kHz}$ is associated to each
 118 RD event.

119 *2.2. Acquisition procedure*

120 Spectra are recorded step-by-step over a 0.3 cm^{-1} interval around the H_2 line with a typical
121 spectral sampling of $5 \times 10^{-3} \text{ cm}^{-1}$. The laser tuning is achieved by changing the voltage applied to the
122 piezoelectric transducer (PZT) inside the ECDL. At each spectral step, the frequency of the laser
123 source is smoothly stabilized thanks to the measured BN frequency and 200 RD events are acquired.
124 About 20 minutes are necessary to record one spectrum in these conditions. A home-made software
125 is then used to average the RD times and associated absolute frequencies, for each spectral step. A
126 flow of high purity H_2 is established in the TS-HFC (Alphagaz 2 from Air Liquide; 99.9999% of purity)
127 to limit the water vapour volume mixing ratio (**Table 1**). Indeed, the $8_{35}-9_{54}$ transition of the v_2+v_3
128 band of H_2^{16}O ($\nu_0 = 4916.9468 \text{ cm}^{-1}$; $S = 8.097 \times 10^{-25} \text{ cm/molecule}$) [4] is slightly interfering with the
129 studied H_2 line. The pressure inside the cell is measured either by a heated absolute capacitance
130 manometer (Model AA02A Baratron from MKS; 1000 mbar full scale; accuracy better than 0.12% of
131 the reading) or an absolute capacitance manometer (Model AA01A Baratron from MKS; 10 mbar full
132 scale; accuracy better than 0.25% of the reading) (**Table 1**). The pressure is regulated with an electro-
133 valve (2871 series from Burkert; 0.3 mm orifice dia.) and a homemade PID software. Series of single
134 spectra recorded for 7 pressure values ranging from 2 Torr to 100 Torr are displayed in **Figure 1**. The
135 temperature measured with an accuracy of 0.04 K was maintained at an almost constant value of
136 $297.43(3) \text{ K}$. Note that on **Figure 1**, we clearly observe that the baseline level of the spectra increases
137 with the pressure (or density) squared due to the underlying collision induced absorption (CIA). The
138 corresponding CIA cross-section will be derived below using the baseline determined during the fit of
139 the S(2) line profile.

140 **Table 1.** Experimental conditions for the different series of spectra of the S(2) 2-0 line of H_2 .

P_{tot} (Torr)	2	5	10	20	50	75	100
# spectra	61	30	55	18	17	57	22
QF ^a	342	515	1350	1604	2599	3419	4067
RMS (cm^{-1})	2.0×10^{-11}	3.3×10^{-11}	2.5×10^{-11}	4.2×10^{-11}	6.6×10^{-11}	7.8×10^{-11}	8.9×10^{-11}
VMR _{H₂O} ^b (ppm)	325.4	129.4	130.8	71.8	54.2	51.4	21.7
Pressure gauge ^c	Gauge #1	Gauge #1	Gauge #2	Gauge #2	Gauge #2	Gauge #2	Gauge #2
Temp. (K)	297.42	297.41	297.41	297.46	297.46	297.40	297.42

141
142 Notes

143 ^a QF (Quality factor) correspond to the ratio of the absorption at the peak to the RMS of the residuals obtained
144 with a qSDNG profile.,

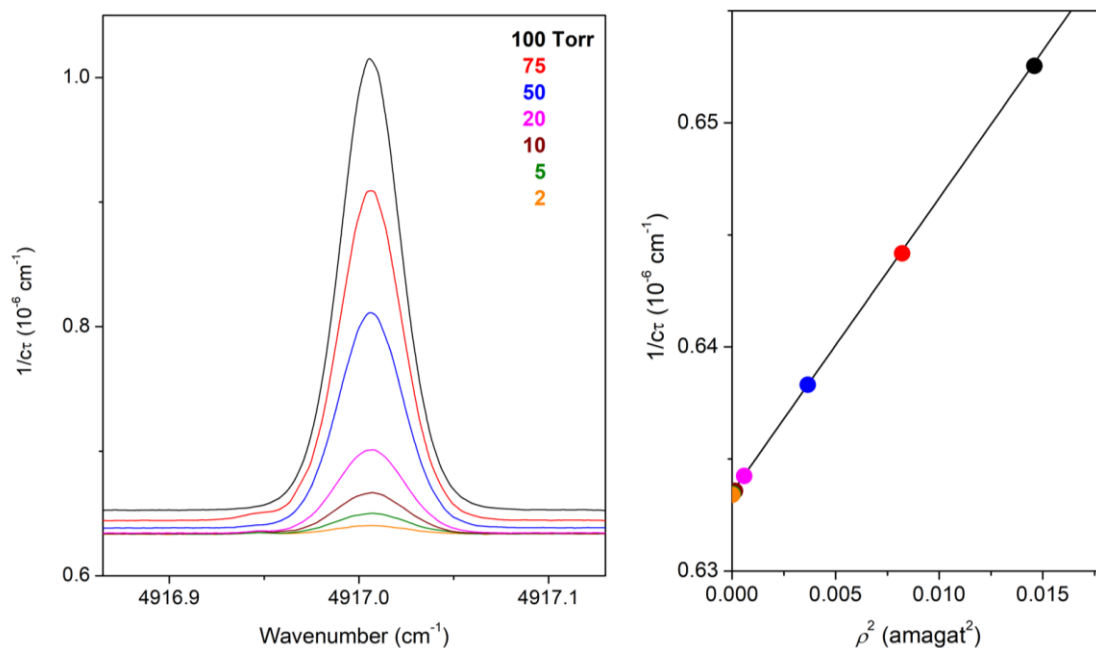
145 ^b VMR: volume mixing ratio

146 ^c Gauge #1: 10 mbar full scale; Gauge #2: 1000 mbar full scale.

147

148 All the spectra recorded for the same pressure value (between 17 and 61 – see **Table 1**) were
149 merged together and averaged by bins. More precisely, over each equally spaced bin of 0.002 cm^{-1} a

150 mean value is calculated for the frequency and the loss rate, $1/\tau$. As a result, seven averaged spectra
151 are obtained for the multi-spectrum fit procedure described below.



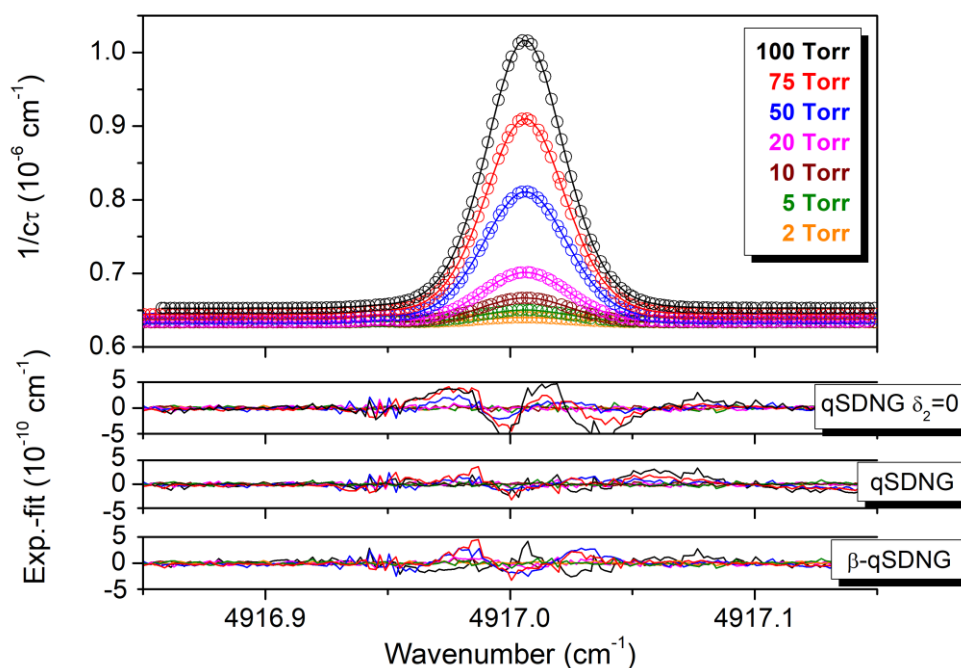
152 **Figure 1.** Overview of the CRDS spectra recorded for the S(2) transition at the different pressures (left panel).
153 Note the increase of the spectrum baseline with the squared density, ρ^2 , due to collisional induced absorption
154 (CIA) of H_2 measured at 4916.860 cm^{-1} (right panel).
155

156 3. Multispectrum fit procedure

157 The frequency of the S(2) transition, ν_0 , is determined from a multi-spectrum fit procedure using
158 the *Multi-spectrum Analysis Tool for Spectroscopy (MATS)* fitting program developed at NIST [17].
159 This procedure is applied to the seven averaged spectra corresponding to the seven pressure values
160 between 2 and 100 Torr. Two different line profiles have been tested:

- 161 (i) A quadratic speed-dependent Nelkin-Ghatak (qSDNG) profile [18] which takes into
162 account the Doppler effect, the collision-induced velocity changes (or Dicke narrowing),
163 quantified by the velocity changing collision rate, ν_{VC} , the collisional broadening and shift
164 and their quadratic speed-dependence. In this profile, the parameter, η , describing the
165 correlation between velocity and internal-states changes in the Hartmann Tran (HT)
166 profile is fixed to zero.
- 167 (ii) A β -qSDNG profile [19,20] for which the Dicke narrowing is treated with an approximation
168 of the billiard ball model [21] including the mass ratio of colliding molecules and the
169 relative importance of speed- and direction-changing collision. This latter profile is
170 supposed to better model molecular systems with large Dicke narrowing such as H_2 and
171 its isotopologues [19].

172 The qSDNG profile is characterized by the transition frequency at zero pressure, ν_0 , the line-
 173 broadening and pressure-shift coefficients (γ_0 and δ_0 , respectively), the Dicke narrowing parameter
 174 (ν_{VC}/P_{tot}), the speed dependence of the pressure-broadening (γ_2) and of the pressure-shift (δ_2), (all in
 175 $\text{cm}^{-1}\text{atm}^{-1}$). In the β -qSDNG profile, ν_{VC} is replaced by $\beta(\chi)\nu_{VC}$ where β is a correction depending of $\chi =$
 176 ν_{VC}/Γ_D . Γ_D is the Doppler width which is fixed to its value calculated at the measured temperature.
 177 During the fitting procedure, the mole fraction of H_2 is fixed to 1 while the integrated intensity of the
 178 $S(2)$ transition is fitted independently for each pressure together with a linear baseline. As already
 179 mentioned, it is necessary to consider the interfering water vapour absorption lines in the fit and
 180 especially the $8_{35}-9_{54}$ transition of H_2^{16}O at $\nu_0 = 4916.9468 \text{ cm}^{-1}$ with a line intensity $S = 8.097 \times 10^{-25}$
 181 $\text{cm}/\text{molecule}$ [4], the other water interfering lines being at least two orders of magnitude weaker.
 182 For that, the water vapour volume mixing ratio is also fitted (**Table 1**) as well as the position,
 183 pressure-broadening and pressure-shift coefficients of the strongest water transition.



184
 185 **Figure 2.**
 186 *Upper panel: CRDS spectra of the $S(2)$ transition of H_2 in the 1-0 band recorded at seven pressure values.*
 187 *Lower panels: Corresponding (exp.-fit) residuals obtained after the multi-spectrum fit procedure using the*
 188 *qSDNG and β -qSDNG profiles.*

189 The results of the multi-spectrum fit procedure obtained with the different profiles are
 190 illustrated on **Figure 2** and the retrieved parameters are reported in **Table 2**. Residuals exceeding the
 191 noise level are observed if the speed-dependence of the pressure-shift is not considered, $\delta_2 = 0$, when
 192 using a qSDNG profile. Improved residuals, but still above the noise level for the four highest
 193 pressures, are obtained both for the qSDNG and β -qSDNG profiles with δ_2 fitted. Contrary to what
 194 could be expected, the latter profile shows no real improvement of the residuals compared to the
 195 qSDNG profile: residuals are slightly better at 100 Torr but larger at 50 and 20 Torr and equivalent for

196 the other pressures. This leads to quality factors between 4067 for the 100 Torr spectrum and 342
 197 for the 2 Torr spectrum (**Table 1**) with the qSDNG profile.

198 **Table 2.** Line shape parameters of the S(2) transition obtained from the multi-spectrum
 199 treatment of the CRDS spectra recorded at seven pressure values using the β -qSDNG, qSDNG profiles.
 200 The uncertainties given within parenthesis in the unit of the last quoted digit correspond to the (1σ)
 201 statistical values provided by the fit. The ab initio absolute frequency value given for the S(2)
 202 transition by the H2spectre software [22]. The ab initio line shape parameters and measured absolute
 203 frequency provided in [6] for the Q(1)(1-0) transition are also listed for comparison.
 204

	ν_0 cm^{-1}	γ_0 10^{-4} cm^{-1} atm^{-1}	δ_0 10^{-3} cm^{-1} atm^{-1}	$\nu_{\text{vc}}/P_{\text{tot}}$ 10^{-2} cm^{-1} atm^{-1}	γ_2 10^{-4} cm^{-1} atm^{-1}	δ_2 10^{-3} cm^{-1} atm^{-1}
Ab initio	4917.006312(33)					
TW β-qSDNG	4917.0063643(41)	11.8(7)	-1.05(4)	1.87(2)	1.25(7)	1.82(11)
qSDNGP	4917.0063637(32)	10.6(6)	-1.04(3)	1.24(1)	1.03(11)	1.76(13)
qSDNGP ($\delta_2=0$)	4917.0063651(56)	10.3(9)	-1.56(5)	1.25(2)	0.96(16)	0
Recommended value	4917.006363(5)^a					
Ref. [6]	4155.253790(10)	6.4(6)	-1.17(12)	4.31(21)	1.06(10)	2.30(22)

205
 206 *Note*
 207 ^a The recommended value is corrected from the recoil and second-order Doppler shifts. The uncertainty includes
 208 all the uncertainty sources discussed in the budget error section.
 209

210 In addition, the CIA can be extracted from the baselines obtained with the multi-spectrum fit
 211 procedure. For this purpose, the loss rate, $1/\tau$, corresponding to the baseline value for the 4916.860
 212 cm^{-1} wavenumber, is plotted versus the squared density in amagat² (**Figure 1**, right panel) and then
 213 fitted with a linear function. The retrieved slope ($1.310(4) \times 10^{-6} \text{ cm}^{-1} \text{ amagat}^{-2}$) at 4916.86 cm^{-1} and
 214 297.43 K is very close (0.7%) to the (calculated) value of $1.319 \times 10^{-6} \text{ cm}^{-1} \text{ amagat}^{-2}$ reported in the
 215 HITRAN2020 database [4] at 4917.00 cm^{-1} and 300 K.

216 4. Budget error

217 More important than the fit residuals, is the statistical uncertainty on the retrieved ν_0 value for
 218 the different profiles and the dependence of ν_0 to the choice of profile. As can be seen from **Table 2**,
 219 the retrieved ν_0 value varies by no more than $6 \times 10^{-7} \text{ cm}^{-1}$ (18 kHz) between the β -qSDNG and qSDNG
 220 profiles, largely within the statistical uncertainty given by the fit (between 100 and 170 kHz according
 221 to the profile). The limited impact of the choice of the profile on ν_0 has already been discussed in the
 222 study of the (2-0) transitions of Ref. [5]. In addition, we see in **Table 2** (as in [5]) that the δ_2 value has
 223 a very limited impact on the retrieved ν_0 value.

224 In Ref. [23], it was shown that the uncertainty on the frequency due to the optical frequency
 225 comb, the Doppler shift induced by the moving speed of the output mirror of the optical cavity and
 226 the AC/DC Stark shifts are well below the kHz level.

227 As mentioned in [24], the *off-diagonal elements relat(ing) to the numerical correlation between*
228 *floated parameters in the fit, (...) are not used in calculation of the standard error* leading to possible
229 underestimation of the «real error». To estimate if this is the case here, we first simulated 100 sets of
230 seven spectra with different random noise and then calculated the standard deviation of the
231 retrieved ν_0 frequency from the multi-spectrum fit procedure. In the typical noise conditions of our
232 recordings (10 kHz on the x -axis and $5 \times 10^{-11} \text{ cm}^{-1}$ on the y -axis), we found that the uncertainty given
233 by the fit for ν_0 (and for δ_0 and δ_2 too) is representative of the « real error ».

234 We also evaluated the impact on ν_0 of the uncertainty given by the fit procedure for δ_0 and δ_2
235 which are the two parameters which are significantly correlated with ν_0 . The fit procedure was run
236 twice: the first one with δ_0 or δ_2 fixed to their fitted values and the second time by fixing them to
237 their fitted values increased by the fit uncertainty. We obtained a variation of $3.0 \times 10^{-6} \text{ cm}^{-1}$ ($\approx 90 \text{ kHz}$)
238 on ν_0 for δ_0 and of $1.8 \times 10^{-6} \text{ cm}^{-1}$ ($\approx 48 \text{ kHz}$) for δ_2 . Note that in the *MATS* program, $a_s = \delta_0/\delta_2$ is the
239 parameter which is fitted instead of δ_2 directly.

240 We proceeded in the same way to evaluate the impact of an error on the position, pressure-
241 broadening and pressure-shift coefficients of the interfering water transition. The fit uncertainty on
242 $\nu_{0\text{-H}_2\text{O}}$, $\gamma_{0\text{-H}_2\text{O}}$ and $\delta_{0\text{-H}_2\text{O}}$ propagates to an uncertainty of $3.3 \times 10^{-7} \text{ cm}^{-1}$, $2.3 \times 10^{-7} \text{ cm}^{-1}$ and $7.4 \times 10^{-7} \text{ cm}^{-1}$
243 on ν_0 , respectively. The retrieved values for $\nu_{0\text{-H}_2\text{O}}$, $\gamma_{0\text{-H}_2\text{O}}$ and $\delta_{0\text{-H}_2\text{O}}$ are $4916.94687(8) \text{ cm}^{-1}$,
244 $0.0591(11) \text{ cm}^{-1} \text{ atm}^{-1}$ and $-0.0074(11) \text{ cm}^{-1} \text{ atm}^{-1}$, respectively. The position value is very close to the
245 value included in the HITRAN2020 database (with a difference of $7 \times 10^{-5} \text{ cm}^{-1}$). The pressure
246 broadening and the pressure-shift coefficients of the considered H_2O line by H_2 are in agreement
247 within the error bars with the values calculated in Refs. [25,26] using the Modified Complex Robert-
248 Bonamy (MCRB) formalism ($0.0695(139) \text{ cm}^{-1} \text{ atm}^{-1}$ and $-0.0082(5) \text{ cm}^{-1} \text{ atm}^{-1}$, respectively).

249 It is also necessary to mention that the R(17)e transition of $^{12}\text{C}^{18}\text{O}^{16}\text{O}$ in the 20012-00001 band
250 ($\nu_0=4916.969519 \text{ cm}^{-1}$; $S=2.431 \times 10^{-24} \text{ cm/molecule}$)[4] is a potential interfering line. To evaluate its
251 potential impact on ν_0 we looked for possible traces of CO_2 in the sounded gas by recording spectra
252 of the stronger P(60) $^{12}\text{C}^{16}\text{O}_2$ line ($\nu_0=4918.07704 \text{ cm}^{-1}$; $S=7.37 \times 10^{-24} \text{ cm/molecule}$) of the 20012-
253 00001 band. No absorption due to this line was observed in our spectra giving an upper limit of 0.25
254 ppm for the CO_2 mixing ratio in our sample. Neglecting the potential presence of 0.25 ppm of CO_2 in
255 our cell (at all pressure values) leads to a bias of $1.7 \times 10^{-6} \text{ cm}^{-1}$.

256 The fitted value of ν_0 needs to be corrected from the recoil shift [27], leading to a reduction of the
257 frequency by -23.9 kHz in our case, and the second-order Doppler shift [28] corresponding to an
258 almost negligible shift of +1 kHz. The recommended absolute wavenumber of the S(2) transition is
259 reported in **Table 2** with a final uncertainty of $5 \times 10^{-6} \text{ cm}^{-1}$ (*i.e.* 150 kHz) corresponding to the
260 quadrature sum of all the different contributions described above.

261 As can be observed on **Figure 2**, residuals are not at the noise level for the highest pressures,
262 showing some limitations of the qSDNGP model. To overcome these limitations and evaluate the
263 impact of the highest-pressure spectra, we removed the 100, 75 and 50 Torr averaged spectra from
264 the multi-fit procedure keeping only the 2, 5, 10 and 20 Torr spectra for the fit. The retrieved ν_0
265 values in both cases are very close to each other: a difference of $1 \times 10^{-6} \text{ cm}^{-1}$ with a qSDNG profile
266 and $2.4 \times 10^{-6} \text{ cm}^{-1}$ with a β -qSDNG profile were observed, largely within the uncertainty of $1 \times 10^{-5} \text{ cm}^{-1}$
267 provided by the fit of the four lowest pressure spectra. In other words, including the highest pressure
268 spectra allows improving the fit uncertainty but does not impact the retrieved ν_0 value.

269

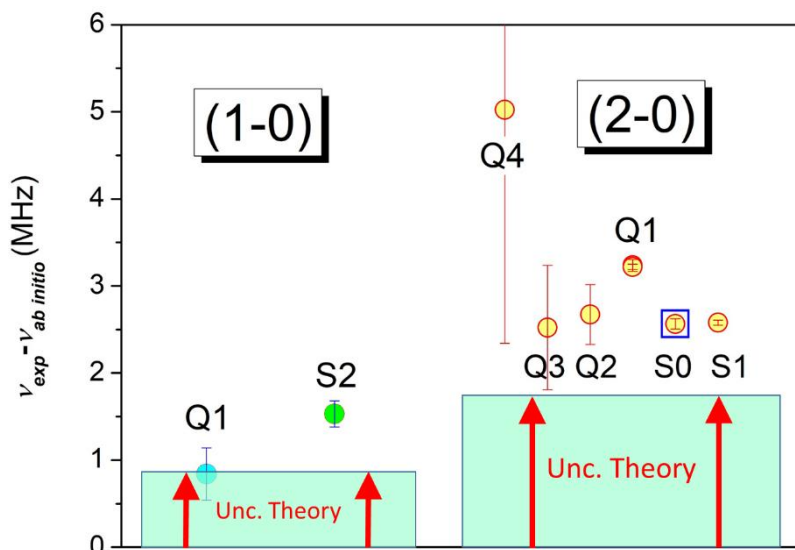
270 5. Discussion and concluding remarks

271 When comparing the *ab initio* values reported in [6] for the Q(1) transition in the 1-0 band of H_2
272 with the fitted line profile parameters obtained for a β -qSDNG profile (**Table 2**), we notice that δ_0 , γ_2
273 and δ_2 parameters are close but the $\nu_{\text{VC}}/P_{\text{tot}}$ *ab initio* value is two times larger than our fitted value.
274 This large difference could be due to the fact that a slightly different profile, including an imaginary
275 part for ν_{VC} , is used in [6]. Finally, the γ_0 *ab initio* value is about two times smaller than our retrieved
276 value. This could come from the fact that these two transitions do not involve the same J values. As
277 observed in [20,29] a J -dependence exists for γ_0 . Indeed, the γ_0 value retrieved for the Q(1) transition
278 is clearly smaller than those reported for other Q transitions measured by Raman spectroscopy in
279 Ref. [29].

280 Even though it was not the initial goal of this work, it is interesting to mention that the integrated
281 intensity of the S(2) transition at 296 K, retrieved from the spectra recorded at the different
282 pressures, show values between 4.567×10^{-27} and $4.579 \times 10^{-27} \text{ cm/molecule}$ (if we except the 10 Torr
283 spectrum for which the pressure value measured with the 1000 mbar gauge leads to a clear outlier
284 with a value of $4.594 \times 10^{-27} \text{ cm/molecule}$). The mean value of $4.572(2) \times 10^{-27} \text{ cm/molecule}$ confirms
285 the *ab initio* intensity value included in the HITRAN database ($4.577 \times 10^{-27} \text{ cm/molecule}$) at the per
286 mil level.

287 In summary, in this work, series of spectra obtained using a highly sensitive CRDS spectrometer
288 linked to an optical frequency comb referenced to a rubidium atomic clock phase-locked to a GPS
289 timing receiver have allowed to determine the frequency of the S(2) transition ($\nu_0 = 147\,408\,142\,357$
290 kHz) with a final uncertainty of 150 kHz. Note that, to the best of our knowledge (see review included
291 in Ref. [30]), the detection of the considered S(2) 1-0 was not reported since the early works by Fink
292 *et al.* [31] and Bragg *et al.* [32] using a grating spectrograph (1.4 km absorption path length) and a
293 Fourier transform spectrometer (path length of 434 m and pressure values between 0.8 and 2.8
294 atm), respectively. With its 150 kHz final uncertainty, the reported transition frequency is the most
295 accurate determination reported so far in the fundamental band of H_2 , improving by more than two

296 orders of magnitude the accuracy of these previous determinations. This is also two times smaller
 297 than the best uncertainty achieved in the fundamental band of H₂ (for the Q(1) transition which is 4.5
 298 times stronger [6]).



299
 300 **Figure 3.** Differences between experiment and theory for the H₂ transition frequencies of the 1-0 and 2-0 bands
 301 referenced to an absolute frequency standard. The theoretical values [1] were obtained from the H2spectre
 302 software [22]. The red arrows represent the typical uncertainty on the calculated values. The experimental
 303 values in the 1-0 band are from Lamperti et al. [6] and this work (Q(1) and S(2), respectively) and from
 304 Fleurbaey et al. [5] for the 2-0 band (yellow dots), the Lamb dip measurement of the S(0) 2-0 frequency is also
 305 indicated (blue open square) [12].

306 The measured value of the S(2) transition frequency is $51 \times 10^{-6} \text{ cm}^{-1}$ (i.e. 1.53 MHz) higher than the
 307 *ab initio* value given by the H2spectre software V7.4 [22]. This difference is 1.5 times larger than the
 308 1 σ -uncertainty reported in [22] and confirms the fact that *ab initio* values are systematically smaller
 309 than experimental ones for H₂ and its isotopologues [5,6,11]. This tendency is illustrated in **Figure 3**
 310 which compares the H₂ transition frequencies of the 1-0 and 2-0 bands referenced to an absolute
 311 frequency standard to the best *ab initio* values [22]. Note that a smaller difference of 0.84 MHz
 312 (equivalent to the *ab initio* error bar) was found by Lamperti and co-workers [6] for the Q(1)
 313 transition belonging to the same 1-0 band of H₂ and given with a 310 kHz uncertainty.

314
 315 **Acknowledgements**

316 The authors are grateful to F. Gibert from LMD and P. Cacciani from PhLAM for lending the
 317 Thulium doped fiber amplifier and the external cavity diode laser, respectively.

- [1] J. Komasa, M. Puchalski, P. Czachorowski, G. Łach, and K. Pachucki, Rovibrational energy levels of the hydrogen molecule through nonadiabatic perturbation theory, *Phys. Rev. A*, **2019**, 100, 032519.
- [2] W. Ubachs, J. C. J. Koelemeij, K. S. E. Eikema, E. J. Salumbides, Physics beyond the standard model from hydrogen spectroscopy, *J. Molec. Spectrosc.*, 2016, **320**, 1–12.
- [3] E. J. Salumbides, J. C. J. Koelemeij, J. Komasa, K. Pachucki, K. S. E. Eikema, and W. Ubachs, Bounds on fifth forces from precision measurements on molecules, *Phys. Rev. D*, 2013, **87**, 112008.
- [4] I. E. Gordon, L. S. Rothman, R. J. Hargreaves, R. Hashemi, E. V. Karlovets, F. M. Skinner, E. K. Conway, C. Hill, R. V. Kochanov, Y. Tan, P. Wcisło, A. A. Finenko, K. Nelson, P. F. Bernath, M. Birk, V. Boudon, A. Campargue, K. V. Chance, A. Coustenis, B. J. Drouin, J.-M. Flaud, R. R. Gamache, J. T. Hodges, D. Jacquemart, E. J. Mlawer, A. V. Nikitin, V. I. Perevalov, M. Rotger, J. Tennyson, G. C. Toon, H. Tran, V. G. Tyuterev, E. M. Adkins, A. Baker, A. Barbe, E. Canè, A. G. Császár, A. Dudaryonok, O. Egorov, A. J. Fleisher, H. Fleurbaey, A. Foltynowicz, T. Furtenbacher, J. J. Harrison, J.-M. Hartmann, V.-M. Horneman, X. Huang, T. Karman, J. Karns, S. Kass, I. Kleiner, V. Kofman, F. Kwabia-Tchana, N. N. Lavrentieva, T. J. Lee, D. A. Long, A. A. Lukashchuk, O. M. Lyulin, V. Y. Makhnev, W. Matt, S. T. Massie, M. Melosso, S. N. Mikhailenko, D. Mondelain, H. S. P. Müller, O. V. Naumenko, A. Perrin, O. L. Polyansky, E. Raddaoui, P. L. Raston, Z. D. Reed, M. Rey, C. Richard, R. Tóbiás, I. Sadiek, D. W. Schwenke, E. Starikova, K. Sung, F. Tamassia, S. A. Tashkun, J. Vander Auwera, I. A. Vasilenko, A. A. Viganin, G. L. Villanueva, B. Vispoel, G. Wagner, A. Yachmenev and S. N. Yurchenko, The HITRAN2020 molecular spectroscopic database, *J. Quant. Spectrosc. Radiat. Transf.*, 2022, **277**, 107949.
- [5] H. Fleurbaey, A. O. Koroleva, S. Kass, and A. Campargue, The high-accuracy spectroscopy of H₂ rovibrational transitions in the (2-0) band near 1.2 μm, *Phys. Chem. Chem. Phys.*, 2023, **25**, 14749-14756.
- [6] M. Lamperti, L. Rutkowski, D. Ronchetti, D. Gatti, R. Gotti, G. Cerullo, F. Thibault, H. Jóźwiak, S. Wójtewicz, P. Masłowski, P. Wcisło, D. Polli and M. Marangoni, Stimulated Raman scattering metrology of molecular hydrogen, *Commun. Phys.*, 2023, **6**, 67.
- [7] F. M. J. Cozijn, P. Dupré, E. J. Salumbides, K. S. E. Eikema and W. Ubachs, Sub-Doppler frequency metrology in HD for test of fundamental physics, *Phys. Rev. Lett.*, 2018, **120**, 153002.
- [8] M. L. Diouf, F. M. J. Cozijn, B. Darquié, E. J. Salumbides and W. Ubachs, Lamb-dips and Lamb-peaks in the saturation spectrum of HD, *Opt. Lett.*, 2019, **44**, 4733.
- [9] M. L. Diouf, F. M. J. Cozijn, K.-F. Lai, E. J. Salumbides and W. Ubachs, Lamb-peak spectrum of the HD (2-0) P(1) line, *Phys. Rev. Res.*, 2020, **2**, 023209.
- [10] T.-P. Hua, Y. R. Sun and S.-M. Hu, Dispersion-like lineshape observed in cavity-enhanced saturation spectroscopy of HD at 1.4 μm, *Opt. Lett.*, 2020, **45**, 4863.
- [11] F. M. J. Cozijn, M. L. Diouf, V. Hermann, E. J. Salumbides, M. Schlösser, and W. Ubachs, Rotational level spacings in HD from vibrational saturation spectroscopy, *Phys. Rev. A*, 2022, **105**, 062823.
- [12] F. M. J. Cozijn, M. L. Diouf, and W. Ubachs, Lamb dip of a Quadrupole Transition in H₂, arXiv:2303.17818v1.
- [13] L. Wolniewicz, I. Simbotin, and A. Dalgarno, Quadrupole Transition Probabilities for the Excited Rovibrational States of H₂, *Astrophys. J. Suppl. Series*, 1998, **115**, 293-313.
- [14] D. Mondelain, A. Campargue, H. Fleurbaey, S. Kass, S. Vasilchenko, Line shape parameters of air-broadened ¹²CO₂ transitions in the 2.0 μm region, with their temperature dependence, *J. Quant. Spectrosc. Rad. Transf.*, 2023, **298**, 108485.
- [15] S. Kass, S. Guessoum, J. C. A. Abanto, H. Tran, A. Campargue, and D. Mondelain, Temperature dependence of the collision-induced absorption band of O₂ near 1.27 μm, *J. Geophys. Res. Atm.*, 2021, **126**, e2021JD034860.
- [16] S. Vasilchenko, T. Delahaye, S. Kass, A. Campargue, R. Armante, H. Tran, and D. Mondelain, Temperature dependence of the absorption of the R(6) manifold of the 2ν₃ band of methane in air in support of the MERLIN mission, *J. Quant. Spectrosc. Rad. Transf.*, 2023, **298**, 108483.
- [17] <https://github.com/usnistgov/MATS>. Doi:10.18434/M32200
- [18] H. Tran, N. H. Ngo, and J.-M. Hartmann, Efficient computation of some speed-dependent isolated line profiles, *J. Quant. Spectrosc. Rad. Transf.*, 2013, **129**, 199-220.
- [19] M. Konefał, M. Słowiński, M. Zaborowski, R. Ciuryło, D. Lisak, and P. Wcisło, Analytical-function correction to the Hartmann–Tran profile for more reliable representation of the Dicke-narrowed molecular spectra, *J. Quant. Spectrosc. Radiat. Transf.*, 2020, **242**, 106784.
- [20] P. Wcisło, I.E. Gordon, H. Tran, Y. Tan, S.-M. Hu, A. Campargue, S. Kass, D. Romanini, C. Hill, R.V. Kochanov, and L.S. Rothman, The implementation of non-Voigt line profiles in the HITRAN database: H₂ case study, *J. Quant. Spectrosc. Radiat. Transf.*, 2016, **177**, 75-91.

-
- [21] R. Ciuryło, D. Shapiro, J. R. Drummond, and A. May, Solving the line-shape problem with speed-dependent broadening and shifting and with Dicke narrowing. II. Application, *Phys. Rev. A*, 2002, **65**, 12502.
- [22] P. Czachorowski, H2SPECTRE version 7.3, Fortran source code, 2020, PhD thesis, University of Warsaw, 2019, <https://www.fuw.edu.pl/Bkrp/codes.html>; <http://qcg.home.amu.edu.pl/H2Spectre.htm>
- [23] H. Fleurbaey, P. Čermák, A. Campargue, S. Kassı, D. Romanini, O. Votava and D. Mondelain, $^{12}\text{CO}_2$ transition frequencies with kHz-accuracy by saturation spectroscopy in the 1.99–2.09 μm region, *Phys. Chem. Chem. Phys.*, 2023, **25**, 16319.
- [24] E. M. Adkins, and J. T. Hodges, Assessment of the precision, bias and numerical correlation of fitted parameters obtained by multi-spectrum fits of the Hartmann-Tran line profile to simulated absorption spectra. *J. Quant. Spectrosc. Radiat. Transf.*, 2022, **280**, 108100.
- [25] C. L. Renaud, K. Cleghorn, L. Hartmann, B. Vispoel, and R. R. Gamache, Line shape parameters for the H_2O – H_2 collision system for application to exoplanet and planetary atmospheres, *Icarus*, 2018, **306**, 275-284.
- [26] R. R. Gamache, B. Vispoel, C. L. Renaud, K. Cleghorn, and L. Hartmann, L., Vibrational dependence, temperature dependence, and prediction of line shape parameters for the H_2O - H_2 collision system, *Icarus*, 2019, **326**, 186-196.
- [27] Z. D. Reed, B. J. Drouin and J. T. Hodges, Inclusion of the recoil shift in Doppler-broadened measurements of CO_2 transition frequencies, *J. Quant. Spectrosc. Radiat. Transf.*, 2021, **275**, 107885.
- [28] Laser Spectroscopy: Vol. 2: Experimental Techniques 4th Edition by Wolfgang Demtröder (Author), Springer Ed.
- [29] L. Rahn, R. Farrow, and G. Rosasco. Measurement of the self-broadening of the H_2 Q (0-5) Raman transitions from 295 to 1000 K, *Phys. Rev. A*, 1991, **43**, 6075–6088.
- [30] A. Campargue, S. Kassı, K. Pachucki, and J. Komasa, The absorption spectrum of H_2 : CRDS measurements of the (2-0) band, review of the literature data and accurate *ab initio* line list up to 35 000 cm^{-1} , *Phys. Chem. Chem. Phys.*, 2012, **14**, 802-815.
- [31] U. Fink, T. A. Wiggins, and D. H. Rank, Frequency and intensity measurements on the quadrupole spectrum of molecular hydrogen, *J. Mol. Spectrosc.*, 1965, **18**, 384–395.
- [32] S. L. Bragg, J. W. Brault, and W. H. Smith, Line positions and strengths in the H_2 quadrupole spectrum, *Astrophys. J.*, 1982, **263**, 999-1004.